Processing of barley grains in a continuous vibrating conveyor

Keppler, S.; Bakalis, S.; Leadley, C.e.; Fryer, Peter

DOI:
10.1016/j.jfoodeng.2016.04.010

Document Version
Publisher's PDF, also known as Version of record

Citation for published version (Harvard):
Keppler, S, Bakalis, S, Leadley, CE & Fryer, P 2016, 'Processing of barley grains in a continuous vibrating conveyor', *Journal of Food Engineering*, vol. 187, pp. 114-123. https://doi.org/10.1016/j.jfoodeng.2016.04.010

Journal of Food Engineering 187 (2016) 114–123

Contents lists available at ScienceDirect

Journal of Food Engineering

journal homepage: www.elsevier.com/locate/jfoodeng

Processing of barley grains in a continuous vibrating conveyor

S. Keppler [a, *], S. Bakalis [a], C.E. Leadley [b], P.J. Fryer [a]

[a] University of Birmingham, School of Chemical Engineering, Edgbaston, Birmingham, B15 2TT, UK
[b] Campden BRI, Gloucestershire, UK

ARTICLE INFO

Article history:
Received 9 October 2015
Received in revised form
8 April 2016
Accepted 13 April 2016
Available online 14 April 2016

Keywords:
Vibrating conveyer
Residence time distributions
Particle flow
Heat transfer

ABSTRACT

A novel tubular industrial apparatus for the surface pasteurization of particles has been studied. Particles are conveyed through a helical pipe by vibrations created by off-balance motors. The residence time of barley grains was characterized. The behaviour of the system was a function of motor angle and motor speed. The residence time could vary up to 21% during one experiment of 2 h (20°, 740 rpm). However, ranges of processing conditions were identified that produce stable operation and thus effective pasteurization of product. In some cases, residence time increased by up to 7% of the initial value over consecutive experiments (40°, 710 rpm). Some reasons for this phenomenon have been proposed and tested. The formation of a powder layer inside the pipe has been proven to affect the residence time of barley grains. A simple model for pasteurization of particles has been developed to characterise the impact of variation in residence time on microbial inactivation.

1. Introduction

Thermal processing is a major part of the food industry; it is carried out for a range of reasons, both to improve product quality but also to enhance the microbiological safety of products. It is essential to ensure that the thermal process does not damage the product. Careful selection of the correct temperature-time combination of the thermal process is thus critical in determining the success of the overall product.

In recent years, foodborne pathogen infections associated with the consumption of low water activity products such as almonds, peanut butter, or powdered infant formula have received increased attention (Beuchat et al., 2013). The primary pathogen of concern is *Salmonella* spp. (Codex Alimentarius Commission, 2013; Beuchat et al., 2011). Between 2000 and 2011, at least 1771 people were affected in Australia, New Zealand, Canada, USA and Europe by outbreaks of such infections (Beuchat et al., 2011). Even though a low water activity generally inhibits microbial growth, cells can remain viable at these conditions (Penaloza Izurieta and Komitopoulou, 2012; Mattick et al., 2000). Additionally, microorganisms can be more resistant to heat in matrices with reduced water activity (Barrile and Cone, 1970; Penaloza Izurieta and Komitopoulou, 2012; Podolak et al., 2010; Villa-Rojas et al., 2013). Depending on food preparation, portion size, and individual circumstances of the consumer, viable pathogenic cells can cause sickness. Consequently, measures like processing interventions that lead to a minimum 4 log reduction of Salmonella in almonds have been adopted to ensure the safety of these products (Almond Board of California, (2007)). Some kinetic data for relevant organisms is given in Table 1.

Technological solutions to the pasteurisation/sterilisation of particulates have focused on steam pasteurisation. This has proven to be more efficient than dry heat in inactivating microorganisms in low water activity, particulate products. Reasons include:

- Steam can penetrate small areas and cavities within the particles. Furthermore, steam has a greater specific enthalpy at 100 °C than water at that temperature and it increases the temperature of the particle's surface rapidly due to steam condensation (Lee et al., 2006).
- Microorganisms are more thermally sensitive at the increased moisture content on the product surface caused by steam condensation (Chang et al., 2010). Proteins are more stable at low water contents in the cells (Podolak et al., 2010; Neetoo and Chen, 2011). Hence, at low water content more energy is needed to unfold the protein structure, which leads to increased heat resistance (Podolak et al., 2010). In comparison, moist thermal treatment potentially destroys the proteins (Neetoo and Chen, 2011). Consequently, disulphide bonds and hydrogen bonds in

* Corresponding author.
E-mail address: sxk250@bham.ac.uk (S. Keppler).

http://dx.doi.org/10.1016/j.jfoodeng.2016.04.010

Table 1
Kinetic data for microorganisms relevant to low moisture products.

Microorganism	Product	D-value [min]	z-value [°C]	Conditions	Source
Salmonella Tennessee	Toasted oat cereal	$D_{85} = 133.9$ $D_{105} = 2.4$	11.86	Dry heat treatment	(Chick, 2011)
Salmonella Agona		$D_{85} = 117$ $D_{105} = 5.2$	14.90		
Salmonella Enteritidis PT 30	Almond flour	$D_{80} = 1.63$	8.28	Dry heat treatment $a_w = 0.610$	(Villa-Rojas et al., 2013)
Salmonella weltevreden	Wheat flour	$D_{60-62} = 875$ $D_{63-65} = 29$	15.2 53.9	Initial $a_w = 0.4$ Initial $a_w = 0.5$	(Podolak et al., 2010)
Salmonella Enteritidis PT 30	Almonds	$D_{60} = 2.6$ $D_{80} = 0.75$	35	Hot water treatment	(Harris et al., 2012)
Salmonella Enteritidis	Almonds	$D_{93} = 0.27$	–	Steam treatment	(Lee et al., 2006)

the surrounding protein weaken and break (Podolak et al., 2010).

The principle of controlled condensation is the base of a steam pasteurisation process. The goals of such a process are:

- The formation of a thin layer of moisture on the surface of each particle;
- Maintenance of those conditions for sufficiently long for the inactivation of pathogens;
- A short drying step in the end of the process to provide a safe, dry, and stable product.

Several methods are used for this purpose (Napasol, 2015; ETIA, 2014; Buhler, 2014). In batch systems, moist heat and reduced pressure are common to ensure high quality and safe products (Napasol, 2015; Buhler, 2014). Continuous systems such as electrical heated screw conveyors are also implemented (ETIA, 2014). The continuous system presented in this study (Revtech, 2015) conveys particles up a helical pipe by vibrations. The pipe is heated directly by resistive heating in which electrical current flows through the pipe at low voltages (approx. 30 V). The combination of the vibrations of the helix and a relatively low bed height of the product are considered to deliver quick and even heat transfer from the heated walls of the pipe to the particles. Steam can be added and extracted at various points throughout the process.

The design of any process to deliver a microbial reduction requires understanding of the variation of residence time of material within the process. In the process studied here, understanding of the particle motion and the accurate predictability of the residence time are critical for the design of a thermal process that results in high quality and safe products. The aims of this study were:

- To investigate the influence of various process parameters on the residence time of barley grains through the equipment, and
- To identify areas where the residence time is stable with time, and
- To develop a theoretical model to estimate the pasteurising effect of the process

Parallel work has studied the use of the device to process flour (Keppler et al., 2015).

2. Materials and methods

2.1. Material

One batch of 200 kg of barley grains was used for the experiments. This was provided by Campden BRI (Gloucestershire, UK).

The median (by volume) of the particle size was calculated to be 5210 ± 430 μm with a sphericity of 0.81 ± 0.01 on a QICPIC system (Sympatec GmbH, D) with a measurable particle size of 30 μm–10,000 μm (Gradis disperser, M9 lense). The bulk density was measured to be 687 ± 2 kg/m^3.

2.2. Equipment

The equipment used for the experiments is a continuous, thermal processing unit provided by Revtech (Loriol-sur-Drôme, France). It consists of three major parts, a hopper, a heating spiral, and a cooling spiral. In this study only the hopper and the heating spiral were used for simplicity. As shown in Fig. 1, particles are conveyed by a screw feeder (B) from the hopper (A) into the spiral. It is a helical, steel pipe (C) with an internal diameter of 84.5 mm, a slope of 2.83° to the horizontal, and a length of approx. 34.4 m. It is possible both to heat the pipe by resistive heating and to inject steam, but in this case, no thermal treatment was applied. The screw feeder speed is controlled by a check-weigher to keep the mass flow constant. This controls the overall particle flow, whilst the behaviour in the tubing is controlled by the vibrations of the motors. Two off-balance motors (D) are attached on opposite sides of the spiral and at an adjustable angle with the horizontal. They create vibrations of different amplitudes and frequencies. The vibrations can be controlled by changing:

- *Motor angle*. The movement of the motor is perpendicular to the motor axis. Adjustment of the motor angle β affects the velocity components of the motors in horizontal and vertical direction. This is shown in Fig. 2 and the components are defined as equations (1) and (2). With increasing angle β, which ranges

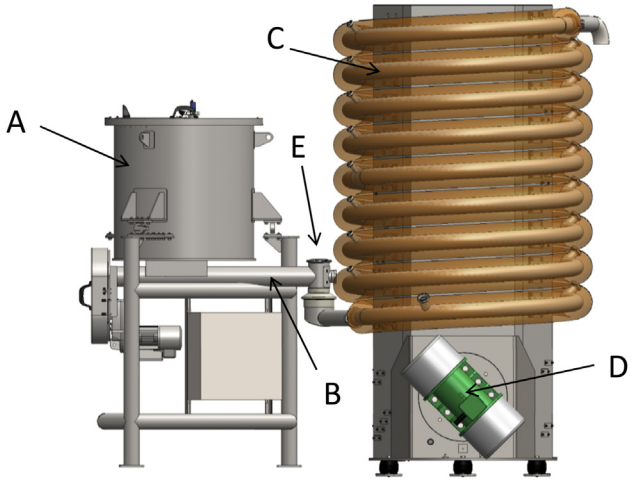

Fig. 1. Experimental setup: Hopper (A), screw feeder (B), insulated helical pipe (C), motor at an angle with the horizontal (D), insertion point for coloured grains (E).

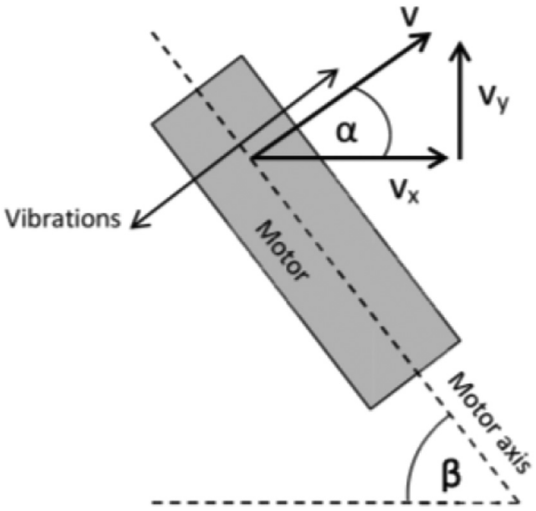

Fig. 2. Relation between total velocity (v) of the motor movement, velocity components in horizontal and vertical direction (v_x, v_y), and motor angle to the horizontal (β).

between 0° and 90° ($\alpha = 90° - \beta$), the horizontal velocity component increases, whereas the vertical one decreases.

$$v_x = v \cdot cos(\alpha) \quad (1)$$

$$v_y = v \cdot sin(\alpha) \quad (2)$$

- *Motor speed*. This controls the vibrational frequency of the oscillations and can be adjusted between 600 rpm (10 Hz) and 740 rpm (12.3 Hz).

The vibrations cause particles to move from the bottom to the top of the spiral. The product exits the helical pipe via a flexible plastic tube that is connected to the top and it is collected in a plastic container.

2.3. Measurement of residence times

The residence time of barley grains was measured by a colorimetric method. Single grains were coloured with a permanent marker and left to dry overnight at ambient conditions. They were then individually added to a constant product flow into the machine (at point E in Fig. 1) and the time was taken with a stopwatch from the time when the grain entered the spiral until it was detected by eye at the exit in the collection container. Grains were added in parallel at approx. 1.5–2 min intervals. Experiments were typically of 2 h duration after which the hopper was empty and the residence time of approx. 55–80 grains was measured per experiment. A constant flow rate was ensured from approximately 5 min after the start of the machine until the end of the experiment.

2.4. Design of experiments

The motor angles of the machine were set to 20°, 30°, and 40°. Preliminary experiments were carried out to identify suitable motor speeds.

- At 20°, no significant differences in residence time could be detected between the minimal and the maximal value of the motor speed range. Hence, no values were tested in between.
- At 30°, the difference between the results at 600 rpm and at 740 rpm was larger and thus, 660 rpm was investigated as well.
- At 40°, different magnitudes as well as dynamics of the residence time were observed depending on the motor speed. An attempt was made to find a motor speed at which the residence time is constant over the entire timescale of the experiment. By trial-and-error method, motor speeds of 600 rpm, 710 rpm, 723 rpm, and 740 rpm were investigated.

The flow rate for all experiments in this study was set using the screw feed to be 100 kg/h. The screw speed is adjusted by a checkweigher to keep the flow rate constant in the hopper as the bulk density decreases. Generally, the pipe was not cleaned between the experiments, but the effect of cleaning is assessed in section 2.5. At least 3 and up to 11 experiments were carried out for each set of processing conditions.

2.5. Identification of stable and unstable residence time

Changes in residence time were investigated during both single experiments as well as over the course of several experiments. This was done to identify time periods when the distribution was stable, and to suggest reasons for any drift.

2.5.1. Single experiment

Different processing conditions resulted in different residence time dynamics over the timescale of one experiment. To characterise stable and unstable periods, two different methods were used.

a. Generally, the residence time data was analysed in Minitab 17®. Control charts in Minitab were used to establish whether the residence time was constant with time. Three standardised tests were applied and if the data failed one of them, the point was taken as transition point or stabilisation time. Here, these tests were:
   - 1 point >3 standard deviations from centre line (overall average of data)
   - 9 points in a row on same side of centre line
   - 6 points in a row, all increasing or all decreasing

The stable subset of the data was tested again. Sporadic outliers were neglected and in case one data set failed one of the tests, but none of the other sets at the same conditions did, it was still pooled to include variability.

b. At motor angles of 40° and motor speeds of 600 rpm and 710 rpm, an initial start-up phase was observed before the residence time stabilised. However, even in the stable phase, the residence time showed a small, but continuous increase. This drift meant that control charts could not be used to find the stable phase, because as the data is not constant, it repeatedly failed the tests. Therefore, the stable phase was taken to be after 2500 s of the experiment.

2.5.2. Multiple experiments

With the aim of presenting the dynamics of the residence time over the course of several experiments, the residence time data of the stable phases of all experiments over one day was connected and plotted versus a cumulative machine run-time. The first point of the stable phase of one experiment was connected to the last point plus 1 s of the stable phase of the previous experiment. Two or three experiments were performed per day. One dataset was created for each set of processing conditions and regressions were

performed in Microsoft Excel (2010).

At 40°, the starting transient of the first 2500 s was removed for all motor speeds to allow data to be better compared. As the residence time was stable at a motor speed of 600 rpm and motor angles of 20° and 30°, all data was used in both cases.

2.6. Statistics

The mean and standard deviation was calculated for the stable phases of at least 3 and up to 11 data sets per processing condition. The results are expressed as mean ± standard deviation. The effect of different runs of the same day could be identified by examining different individual data sets.

Different data sets at the same processing conditions were generally not identical as proven by an analysis of variance (data not shown). Still, the data was pooled and thus, the variability between experiments was included in the results. However, due to the differences between the individual data sets, overall residence time distributions (RTD) were not created.

3. Results and discussion

The particles travel through the vibrating system at a flow rate of 100 kg/h in a homogenous layer with a bed depth of about two particles, with a surface length of 4–5 cm across the pipe. The particles do not fill the pipe; they only bounce a few millimetres high. At a setpoint of 100 kg/h, the flow rate at the inlet of the spiral is accurately controlled at 99.5 ± 1.0 kg/h, which is measured by a checkweigher. The flow rate at the outlet was measured to be 99.2 kg/h ± 0.98 kg/h by collection of product for 60 s over runs of 2 h and weighing it. Control charts in Minitab confirmed no increasing or decreasing trend of the flow rate with time.

The average residence times of the stable phases of various processing conditions are depicted in Table 2 and will be discussed below. Typical experiments involved more than 150 passes of tracer and measurement of the residence time to accuracy of ± 1s. It is possible therefore to identify the RTD to considerable accuracy. For example, Fig. 3a shows the residence time distribution of barley grains (723 rpm, 40°) with a fitted normal distribution. The probability plot indicates that deviations from Normality are small. However, the observed shift in residence times over time discussed below skews the overall distribution and hence, plotting RTDs is not appropriate for all processing conditions.

Experiments were performed at ambient temperatures. At elevated temperatures, moisture migrates from the product into the atmosphere of the pipe. Many properties of the particles are thereby affected (e.g. surface properties, density, coefficient of restitution). It also renders the air more conductive and reduces electrostatic effects. Therefore, it is difficult to predict the effect of temperature on the residence time. This needs to be determined in future studies.

Note that the experiments were performed on a pilot plant device and the results do not directly apply to industrial machines.

Table 2
Mean residence times in seconds of the stable phases at motor angles of 20°, 30°, and 40° and motor speeds between 600 rpm and 740 rpm.

		Motor angle [°]		
		20	30	40
Motor speed [rpm]	600	389 ± 10	298 ± 6	306 ± 13
	660	–	297 ± 6	–
	710	–	–	332 ± 8
	723	–	–	244 ± 6
	740	406 ± 13	261 ± 6	195 ± 3

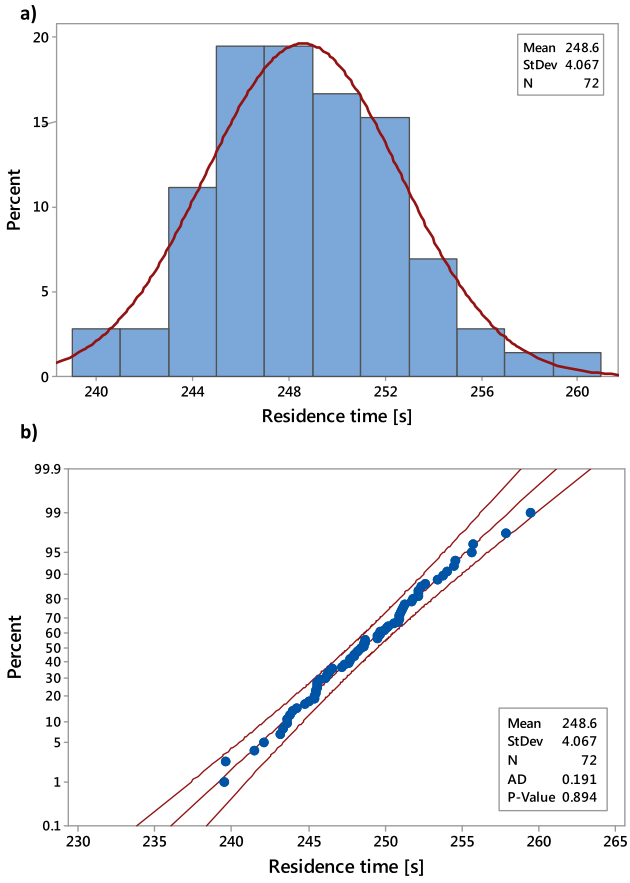

Fig. 3. a) Residence time distribution of barley grains at a motor speed of 723 rpm and a motor angle of 40° and overlaid normal distribution. b) Probability plot with 95% confidence intervals.

3.1. Effect of motor speed

The motor speed relates to the vibrational frequency of the spiral and it is associated with the amplitude of the vibrating bed. The spiral drives the particle flow to vibrate with the maximum amplitude at its resonance frequency. Macroscopically, it can be observed that at some frequencies, the flow is homogenous and regular and at others, the particle bed does not move as one and the flow looks chaotic. The motor speed affects the mean residence time, but as it is constant over time (data not shown) it is not responsible for changes in residence time over time.

The causes for the development of the residence time over time can be divided in.

i) A characteristic time after the start of the machine for the system to stabilise as a function of motor speed and motor angle
ii) Other effects like electrostatic forces that cause the residence time to shift after the stabilisation time.

3.1.1. Motor angle 20°

Fig. 4a shows the residence time of barley grains at motor angles of 20° for motor speeds of 600 rpm and 740 rpm. Time 0 corresponds to the instant where the equipment is turned on. The residence time is plotted against the time instant that the coloured grain enters the system. At 600 rpm, the residence time is stable over the timescale of the experiment as proven with control charts in Minitab (cf. section 2.5). In contrast at 740 rpm, the residence

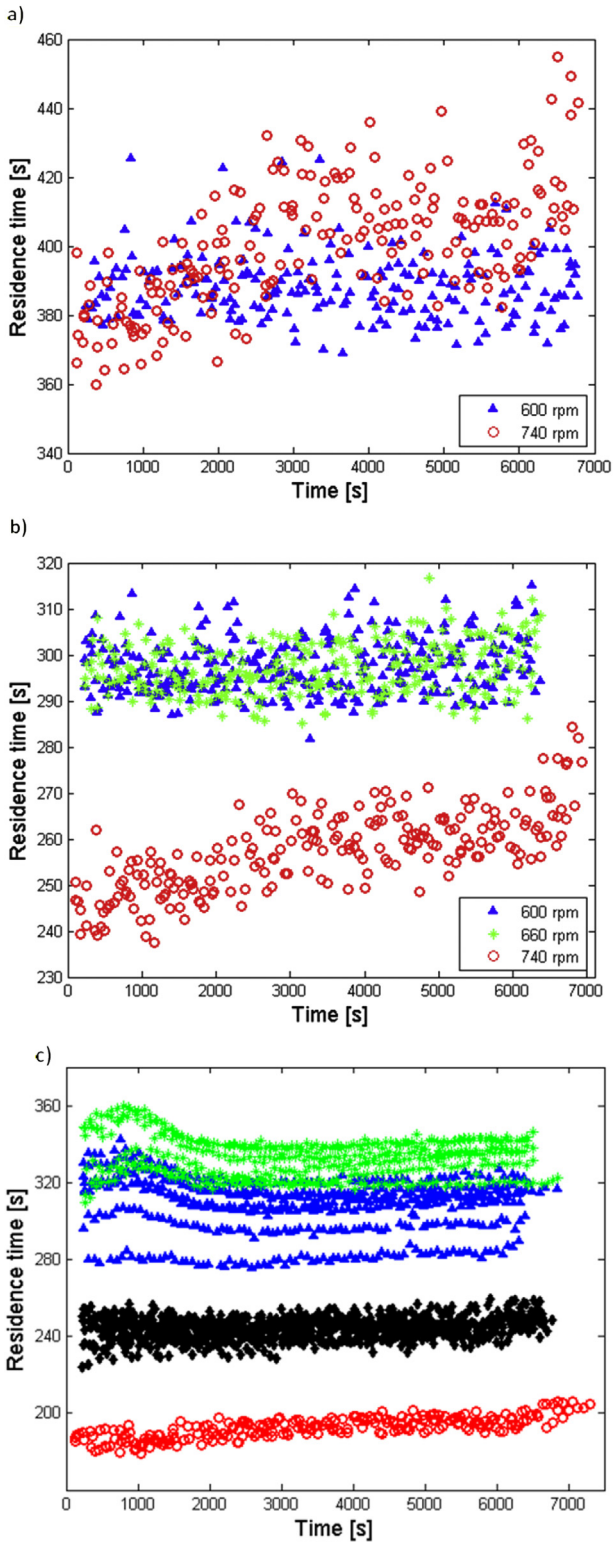

Fig. 4. Residence time of barley grains: a) Motor angles of 20° and motor speeds of 600 rpm and 740 rpm b) Motor angles of 30° and motor speeds of 600 rpm, 660 rpm, and 740 rpm. c) Motor angles of 40° and motor speeds of 600 rpm, 710 rpm, 723 rpm, and 740 rpm (Triangle: 600 rpm. Asterisk: 710 rpm. Diamonds: 723 rpm. Circle: 740 rpm.).

time initially increases then it stabilises before increasing again in the very end. The duration of the initial phase was determined with control charts. In three experiments, it took on average 1937 ± 146 s for the system to stabilise. The stable phase then lasted for 4529 ± 117 s. The variation in residence time between the smallest and the largest measured value was approx. 21.5% (79 s) (3 experiments). This is significantly higher than the standard deviation of 13 s for the stable phase and demonstrates the importance of identifying stable and unstable phases.

The mean residence time is 389 ± 10 s at 600 rpm and 406 ± 13 s at 740 rpm (cf. Fig. 4a). This is calculated from all the data at 600 rpm and from the data for the stable system at 740 rpm. There is only a slight difference of the mean residence time over the motor speed range (<4.4%).

The effect of the motor speed at angles of 20° is predominantly on the dynamics of the system rather than on the magnitude of the residence time. The stable data at 600 rpm facilitates the design of a thermal process. The difference between the average residence times at both motor speeds is small.

3.1.2. Motor angle 30°

The influence of the motor speed at motor angles of 30° is presented in Fig. 4b. Motor speeds of 600 rpm, 660 rpm, and 740 rpm were tested. At 600 rpm and 660 rpm the residence time is stable over the timescale of the experiment, whereas at 740 rpm it increases in the beginning of the experiment before it levels off and increases again in the end. The transition between initial and stable phase was found at 2452 ± 260 s and the duration of the stable phase was 4208 ± 259 s. In three experiments, the variation between the smallest and the largest measured value was approx. 17% (40 s), which is comparable to the results at 20°.

In contrast to motor angles of 20°, different motor speeds also result in different magnitudes of the residence time. For 600 rpm and 660 rpm, the behaviour was not a function of time and average residence times of 298 s ± 6 s and 297 s ± 6 s were measured. However, at a motor speed of 740 rpm, the residence time of the stable phase was determined to be 261 s ± 6 s.

3.1.3. Motor angle 40°

Motor speeds of 600 rpm, 710 rpm, 723 rpm, and 740 rpm were tested for motor angles of 40°. Results are depicted in Fig. 4c. It was found empirically that only at 723 rpm was the residence time approximately constant over the timescale of the experiment. For the other investigated motor speeds, there is an initial, unstable phase before the residence time stabilises. At 600 rpm and 710 rpm, the residence time increases and decreases before it levels off. At 740 rpm, it increases, levels off and increases again in the end of the experiment. In this case, it took 2495 ± 190 s for the system to stabilise and the stable period lasted for 4840 s ± 364 s. The variation in residence time between the smallest and the largest measured value was approx. 12% (22 s) (3 experiments).

By comparison to motor angles of 20° and 30°, changing the motor speed at 40° had a significant effect on the residence time. The mean was measured to be 306 ± 13 s, 332 ± 8 s, 244 ± 6 s, and 195 ± 3 s for motor speeds of 600 rpm, 710 rpm, 723 rpm, and 740 rpm, respectively. With the exception of 600 rpm, the mean and standard deviation decrease with increasing motor speeds of 710 rpm, 723 rpm, and 740 rpm. In this narrow range of motor speed, the residence time decreases by approx. 137 s (41%). It is worth mentioning that the decrease in standard deviation was observed for the pooled data. The standard deviation of the individual data sets was similar for all motor speeds (2 s, 3 s, 4 s, 3 s for 600 rpm, 710 rpm, 723 rpm, 740 rpm). This indicates that the variability between experiments was higher for lower motor speeds, but the dispersion of the grains during each experiment was comparable.

3.2. Effect of motor angle

3.2.1. Motor speed 600 rpm

Fig. 5a depicts the residence time of barley grains at a motor speed of 600 rpm for motor angles of 20°, 30°, and 40°. For 20° and 30°, it is constant over the timescale of the experiment as identified with control charts, whereas at 40° it increases and decreases in the initial phase before it stabilises.

Values of mean residence time distributions of 389 ± 10 s, 298 ± 6 s, and 306 ± 13 s were measured for motor angles of 20°, 30°, and 40°. While the data for 30° and 40° is in a similar range, residence time is about 29% higher for motor angles of 20°. There is no trend in the overall standard deviation from the pooled data sets. However, the standard deviation of the individual data sets decreases with increasing motor angle (data not shown). This demonstrates that the dispersion of the barley grains decreases with increasing motor angle, but the variability between experiments increases.

3.2.2. Motor speed 740 rpm

The influence of the motor angle at a motor speed of 740 rpm is presented in Fig. 5b. At all three angles, there is an initial stage where the residence time increases. It stabilises subsequently and increases again in the end. The stabilisation times were found by means of control charts and determined to be 1937 ± 146 s, 2452 ± 259 s, and 2495 ± 190 s for motor angles of 20°, 30°, and 40°. The duration of the stable phases was 4529 ± 117 s, 4208 ± 259 s, and 4840 ± 364 s for motor angles of 20°, 30°, and 40°. The overall residence time range between maximal and minimal value calculated from three experiments each is 22%, 17%, and 12% from the minimal value for 20°, 30°, and 40°. It shows that the overall variation of the residence time decreases with increasing motor angle.

The results of the pooled data of the stable phases are 406 ± 13 s, 261 ± 6 s, and 195 ± 3 s for motor angles of 20°, 30°, and 40°. The residence time at 20° is approx. 109% higher than at 40° which illustrates the importance of the effect of the motor angle. It is visible that mean and standard deviation decrease with increasing motor angle. This is also true for the individual data sets.

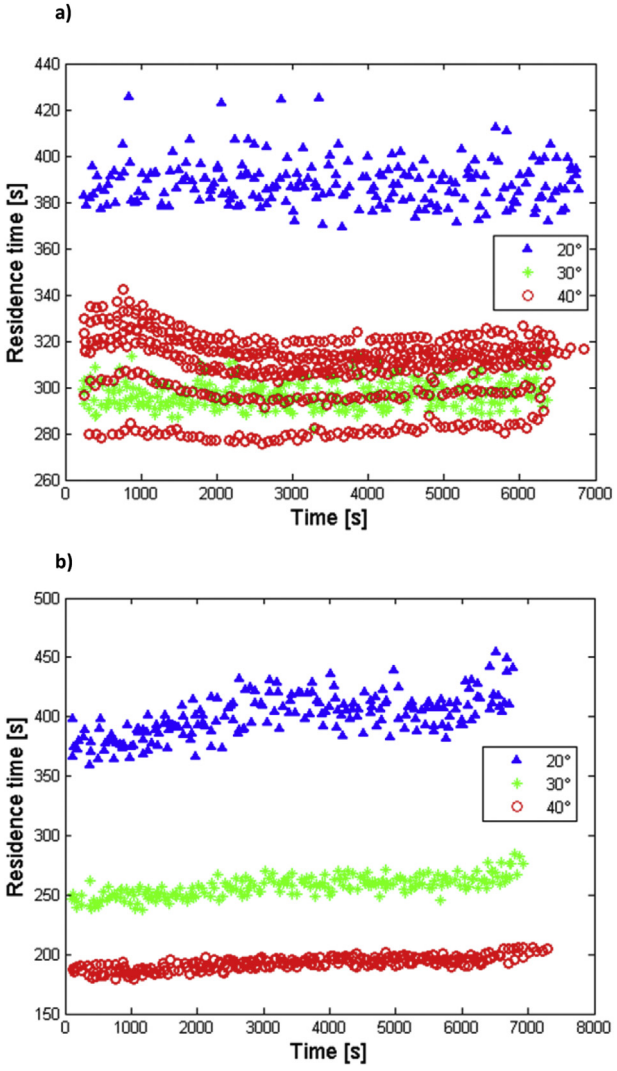

Fig. 5. Residence time of barley grains: a) Motor speed of 600 rpm and motor angles of 20°, 30°, and 40°. b) Motor speed of 740 rpm and motor angles of 20°, 30°, and 40°.

3.3. Summary of effects

For each motor angle, at least one motor speed was found at which the residence time of barley grains was constant over the entire timescale of the experiment. It would thus be possible to define a combination of angle and speed to deliver a uniform process.

At motor angles of 20° and 30°, the motor speed affected the dynamics of the system rather than the magnitude of the residence time; however motor speed at 40° influenced both the mean and standard deviation to a much greater extent. It was also observed that the variability between experiments was higher at lower motor speeds for angles of 40°.

The effect of the motor angle on the average residence time is more significant at 740 rpm than at 600 rpm. A constant residence time was only observed at 600 rpm and motor angles of 20° and 30°. The standard deviation of the individual data sets and therefore the dispersion of the barley grains during one experiment generally decreased with increasing motor angle.

3.4. Residence time dynamics

It was found that under some conditions the residence time evolved over the course of several test runs. Such behaviour might

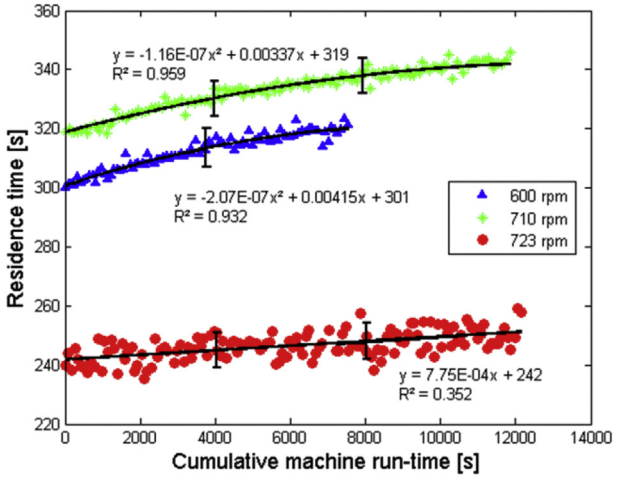

Fig. 6. Development of the residence time of barley grains during the course of a day at motor angles of 40° and motor speeds of 600 rpm, 710 rpm, and 723 rpm. The vertical line indicates the connection points between consecutive experiments.

make it difficult to specify a thermal process. For example, Fig. 6 describes the dynamics of the residence time during the day for motor angles of 40°. Results are given to three significant figures. The stable phases of all experiments during one day were connected. Each experiment took approx. 2 h and subsequently, the data of 2 (600 rpm) or 3 (710 rpm, 723 rpm) experiments was connected. Residence time at 600 rpm and 710 rpm increases with time and follows a quadratic curve quite accurately. At 723 rpm, the data is more scattered and the increase is smaller. In this case, the data can be approximated by a linear equation. Over 12,000 s, the average residence time increases by 19.6 s, 23.2 s, and 9.3 s which is 6.5%, 7.3%, and 3.9% of the initial value for motor speeds of 600 rpm, 710 rpm, and 723 rpm. The fitted curves were used for these calculations; at 600 rpm it was extrapolated. The change in residence time results in a change in particle holdup in the pipe. Only a small change in holdup is needed. The residence time in Fig. 6 increases from approximately 320 s–340 s over a time period of 12,000 s at a motor speed of 710 rpm. At a flow rate of 100 kg/h, this means a change of particle holdup in the pipe of 0.5 kg from ca. 8.9 kg–9.4 kg and a change in flow rate of 0.15 kg/h. Therefore, the change in holdup in the pipe is smaller than the accuracy at which the flow rate can be measured.

The residence time also increased during the day at motor angles of 20° and 30° at 600 rpm (data not shown). The extent of the linear increase was 4.5 s and 4.3 s after 12,000 s, which represents 1.2% and 1.4% of the initial value at motor angles of 20° and 30°, respectively. This data was calculated from the regression curve.

The data indicates that the increase of the residence time at motor angles of 20° and 30° is negligible, whereas it is much more significant at 40°. Furthermore at 40°, it increases to a higher extent at motor speeds of 600 rpm and 710 rpm than at 723 rpm.

Several factors might affect the residence time.

i) *Product effects*. The formation of a thin powder layer inside the pipe due to damage of the product may influence friction or the coefficient of restitution.
ii) *Machine effects*. These could include warming up of the motors, the suspensions or other parts might have an impact on the vibrations over time and hence on the residence time of the grains.
iii) *Environmental parameters* like ambient temperature and humidity might have an influence. In preliminary experiments, no effect of ambient temperature could be found in the process range of 16–24 °C.

These hypotheses were tested at motor angles of 40° and a motor speed of 600 rpm. It would be interesting to study why that increase only occurs at certain conditions and to variable extents. This is to be investigated in future work.

3.4.1. Hypothesis (i): deposition of a powder layer inside the pipe

To test the hypothesis whether the formation of a powder layer inside the pipe due to material damage causes the residence time to increase during the day, a cleaning experiment was performed.

i) Two experiments (2 h each) were performed per day for four consecutive days. At the end of each day, the pipe was cleaned with a cleaning pig and water. The data is shown in Fig. 7a. The first and second runs of all four days fall into two repeatable groups. The residence time increases over the course of each day as it is clearly higher in the second run than in the first one.
ii) Two experiments (2 h each) were performed per day for two consecutive days without cleaning the pipe. This is shown in Fig. 7b. The first and second run of the first day match the data in Fig. 7a. However, on the second day, the residence time of the first run is higher than that of the first run of the first day, but the second run on the second day behaves identically to that on the first day.

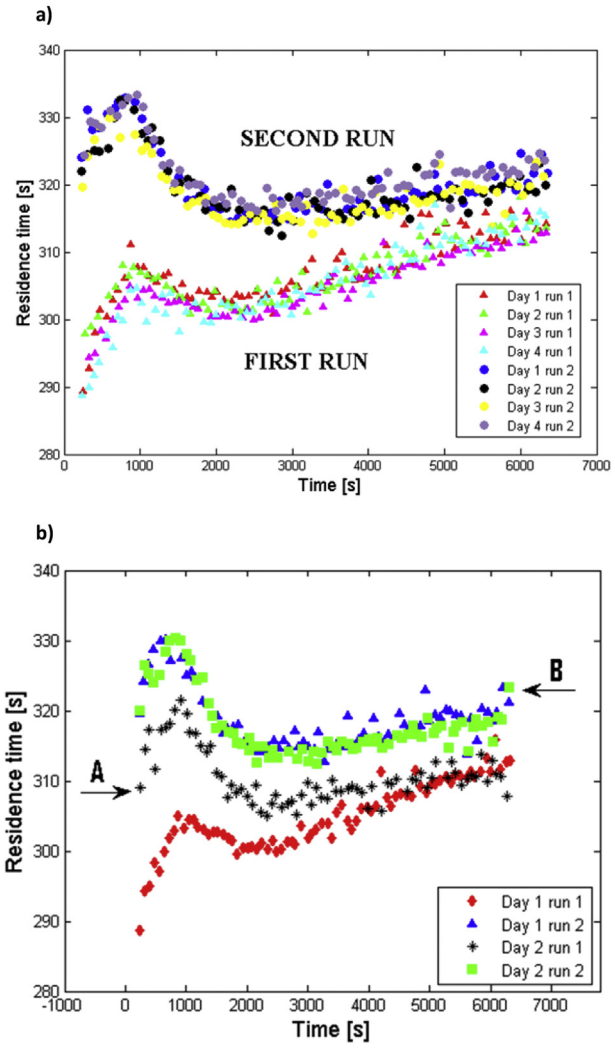

Fig. 7. a) Residence time of barley grains at motor angles of 40° and a motor speed of 600 rpm at four consecutive days (2 runs each day). Cleaning after each day. b) Residence time of barley grains at motor angles of 40° and a motor speed of 600 rpm at two consecutive days (2 runs each day). No cleaning.

Hence, it is obvious that the cleaning has an influence on the residence time. Without the cleaning, the residence time appears to increase.

On the other hand, if the residence time was solely due to the powder layer, it might be expected that the residence time at the start of the second day (point A in Fig. 7b) would be the same as at the end of the previous day (point B in Fig. 7b). However, the start point for the residence time decreases, perhaps due to alterations in the powder layer over night, e.g. humidity loss or gain or electrostatic charging. The experiments show that the formation of a powder layer inside the pipe affects the residence time of barley grains; more work would be needed to identify the precise cause.

3.4.2. Hypothesis (ii): warming up of the machine

The possible effect of warming up of the motors or other parts of the machine on the residence time of barley grains was tested. The machine was run for the period of one experiment (2 h) without

product to exclude product effects. Subsequently, product was added and two more experiments were performed. The data can be compared to days where the machine was started with product from the beginning and two experiments were completed.

The results are presented in Fig. 8 and show that data for experiments run after 2 h of operation are identical to data from the first and second experiments of the control days. If the warming up of the motors caused the increase of the residence time the two data sets would be different.

Hence it is concluded that the vibrations are controlled accurately and the warming up of the machine does not influence the residence time of barley grains.

4. Model development for process validation

The work above has demonstrated a wide range of residence times of barley grains for different processing conditions. It is unclear whether the observed variations are of practical significance. To assess this issue, a model was developed that calculates the pasteurisation effect of the process as it is needed for example for the pasteurisation of almonds (Almond Board of California, (2007); Silva and Gibbs, 2012).

Three inputs are required for the model:

i) Residence time distributions
ii) Temperature profiles along the axial direction of the pipe
iii) Microbial inactivation parameters

The residence time data from the experiments described in the previous sections were used as the basis for the model.

The temperature profiles along the axial direction of the pipe are determined by 8 temperature probes embedded between the outside of the steel pipe and the insulation layer. One probe is located in each loop, starting from half a loop after the inlet of the spiral to probe 8 towards the top of the spiral. As the pipe is heated via resistive heating and is open to atmosphere, the temperature is not constant over the total length of the pipe. The temperature is controlled so that at least one of the probes is held at the temperature setpoint, whereas the temperature of the other probes depends on product flow rate and thermal properties of the product. Fig. 9 shows a measured temperature profile for electrical heating

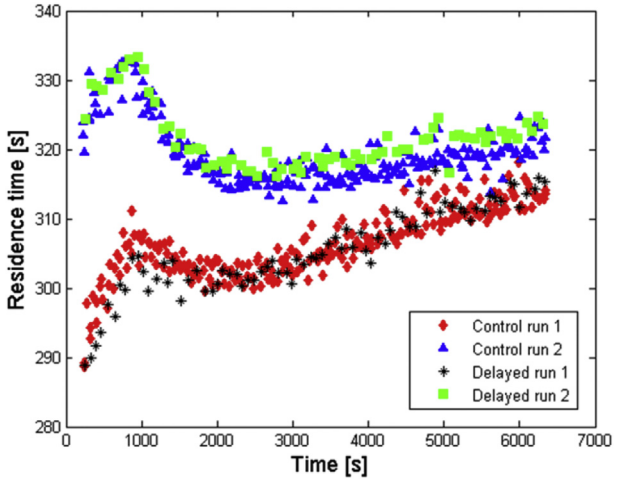

Fig. 8. Residence time of barley grains at motor angles of 40° and a motor speed of 600 rpm. Two sets are shown (i) control run 1 and 2 where the machine was started at the start of run 1 and (ii) delayed run 1 and 2 where the machine was run for 2 h without product before the start of run 1.

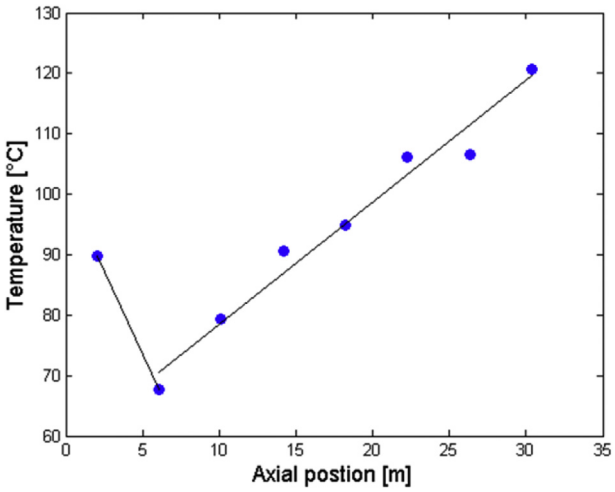

Fig. 9. Temperature profile along axial direction of the pipe. Setpoint 120 °C.

for a setpoint of 120 °C. The temperature profile down the tube is clear. Straight line fits were drawn (i) between the first two temperatures, and (ii) to represent the mean of subsequent temperature probes. This profile is then used in the model as defined below.

The microbial input data comprises the D-value, its reference temperature, and the z-value. These are highly dependent on the microorganism and its environment and furthermore the processing history and the processing conditions (Silva and Gibbs, 2012; Podolak et al., 2010). Candidate organisms and their thermal behaviour are given in Table 1. As an example *Salmonella* Tennessee with $D_{105} = 2.4$ min and $z = 11.9$ °C relevant to particulate grains is used.

D-values and reaction rates are calculated at each temperature in the observed range. The model assumes that the temperature of the surface of the particles is the same as the temperature profile of the probes and that only the surface is microbiologically contaminated. No fitted continuous distribution or minimum residence time was used because of the observed shift in residence time over time. The residence time data is used to calculate the velocity of individual particles. The survivors are determined by the general expression for microbial evolution and the log reductions are established.

The model calculates the thermal process by the following:

1) The D-value is calculated for the observed range of temperatures by linear regression and by means of the z-value.
2) Reaction rates (k(T)) are calculated for the observed range of temperatures.

$$k(T) = \frac{2.303}{D(T)} \cdot \frac{1}{60} \quad [1/s] \tag{3}$$

3) Particles are assumed to travel at constant velocity, calculated by dividing the pipe length by the observed residence time.
4) The pipe length is divided in 344 small segments, each 0.1 m long.

The residence time that a particle takes to pass one segment (Δt) is calculated by dividing the segment length by the velocity.

5) The temperature profile in the axial direction of the pipe is determined from the linearised temperature profile shown in Fig. 9.

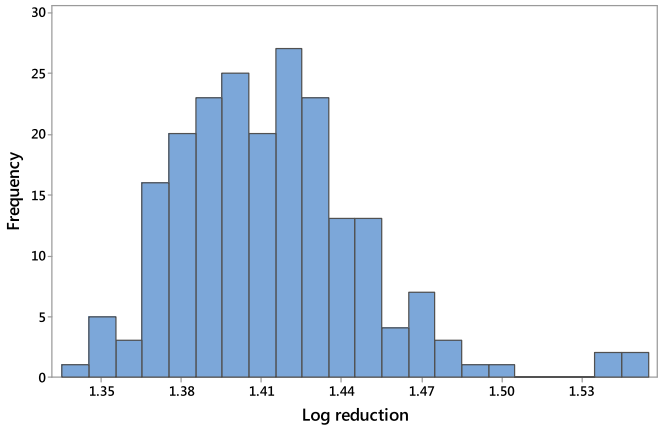

Fig. 10. Distribution of log reductions of S. Tennessee (D_{105} = 2.4 min, z = 11.86 °C) at motor angles of 20° and a motor speed of 600 rpm and a temperature setpoint of 120 °C.

6) The reaction rate is next found for each segment depending on the calculated temperature.
7) The integral $\int 10^{T-T_{ref}/z}dt$ which describes the inactivation effect can be approximated using the temperature profile and section residence time (Heldman, 2011). The fractional microbial kill in each segment is calculated by applying the exponential function to the product of residence time per segment and reaction rates (Heldman, 2011).

$$S_{Segment} = \frac{N_{Segment,outlet}(t)}{N_{Segment,inlet}} = \exp(k(T)\cdot\Delta t) \quad (4)$$

The survivors of all segments are combined by multiplying the sequence.

$$S_{total} = \prod S_{segment} \quad (5)$$

8) The overall log-reduction is calculated

Microbial reduction should be calculated individually for each application. As an example Fig. 10 shows for motor angles of 20° and a motor speed of 600 rpm (data of Fig. 5a), assuming microbiological parameters of D_{105} = 2.4 min and z = 11.86 °C for *Salmonella* Tennessee (cf. Table 1) and the temperature profile of Fig. 9, microbial reduction varies between 1.34 and 1.55 log reductions (overall mean calculated from RTD: 1.41 log reductions).

It is evident that the variation in residence time relates to the microbial reduction linearly. In this case, the residence time ranges between 369 s and 426 s with a mean of 389 s. The difference between minimal and maximal value is 15% for the residence time as well as the microbial log reduction.

Table 3 shows both the mean and the range of microbial inactivation for different motor angles and motor speeds. The highest inactivation results from the highest residence time (motor angles of 20° and a motor speed of 740 rpm) whilst the smallest was calculated for the shortest residence time (motor angles of 40° and a motor speed of 740 rpm). The table also shows the relative differences in microbial inactivation as well as in residence times with respect to their means at all tested processing conditions. The most precise treatment is achieved at 40° and 740 rpm (spread of 9%), but this might be different when individual runs are considered rather than the entirety of all experiments. In contrast, the highest spread was observed for 40° and 600 rpm (19%).

To improve the model and to make it more realistic, the following changes could be made:

i) More complex heat transfer models can be chosen and additionally convection and steam may be taken into account.
ii) Dynamic D-values depending on the water status at the surface of the particles may be included (Jeong et al., 2009).
iii) A more accurate measure of the distribution of temperature across the probes is needed, together with the relationship between wall and particle temperature.

The calculations serve to assess the impact of the variation in residence time on microbial inactivation. An arbitrary model organism was chosen and the model does not reflect the possible magnitude of microbial reduction achievable with the machine; for example the D-value changes significantly as soon as steam is added. The Revtech equipment has been validated for a number of applications with a kill of well over 5 log reductions of *Enterococcus faecium*. The narrower the residence time distribution, the smaller the variation in log reduction will be.

The mass holdup in the system is obviously important in the determination of the residence time. The holdup can be calculated as (flowrate × residence time) assuming no dead spaces and is in the region of 9 kg. The change in holdup that gives rise to the changes in residence time is small (ca. 0.5 kg). All of this work has used a flow of 100 kg/h, and was designed to demonstrate the use of the device. Careful experiments would be needed to confirm the residence time in practice, and to ensure minimal drift in the process time. The methods described here would be useful for such determination. The drift in residence time is less for barley than for flour (Keppler et al., 2015); different particles will show different effects.

5. Conclusion

A novel tubular apparatus for the pasteurisation of particles was investigated. The residence time was characterized in both single experiments and over the period of multiple experiments. The

Table 3
Table of (i) Mean log microbial reductions and (ii) Range of log reductions; difference between maximum and minimum, written as % (range/mean).

		Motor angle [°]					
		20		30		40	
		Mean [log]	Range [%]	Mean [log]	Range [%]	Mean [log]	Range [%]
Motor speed [rpm]	600	1.41	15.7	1.08	11.7	1.11	19
	660	–	–	1.08	10.6	–	–
	710	–	–	–	–	1.21	9.6
	723	–	–	–	–	0.89	14.6
	740	1.48	17.7	0.95	13.5	0.71	9

behaviour of the system was a function of two variables, motor angle and motor speed.

At motor angles of 20° and 30°, the motor speed affected the dynamics of the system rather than the magnitude of the residence time; at 40° it influenced the mean and standard deviation to a much bigger extent. At least one motor speed was found for each motor angle at which the residence time was constant over the entire timescale of the experiment. Additionally, it was observed at angles of 40° that the variability between experiments was higher at low motor speeds.

The effect of the motor angle on the average residence time was more significant at a motor speed of 740 rpm compared to 600 rpm. At 600 rpm the residence time was constant for motor angles of 20° and 30° in contrast to 40°, where an initial unstable phase occurred. Unstable dynamics were observed at 740 rpm for all motor angles. The standard deviation of the individual data sets and therefore the dispersion of the barley grains during one experiment decreased with increasing motor angle.

Generally, the residence time increased during the course of the day. The data suggests that the increase of the residence time at motor angles of 20° and 30° is negligible, whereas it is much more significant at 40°. Furthermore, at 40° it increases to a higher extent at motor speeds of 600 rpm and 710 rpm than at 723 rpm. The change is difficult to detect by measuring flow rate – holdup changes by less than a kg over several hours.

Some reasons for this phenomenon were proposed and tested. The formation of a powder layer inside the pipe has proven to affect the residence time of barley grains. It is unlikely that this is the only factor causing the residence time to increase during the day and it is suggested that the properties of that layer might change over time. The warming up of the machine does not influence the residence time. No correlation was found between ambient temperature and residence time.

A simple model for pasteurisation of particles has been developed that characterises the impact of the variation in residence time on microbial inactivation. Across all tested processing conditions, the variation between minimal and maximal log reduction was between 9% and 19%. In this way, precise treatments can be identified.

More work is needed to identify the cause of the drift in residence time, and to confirm or develop the mathematical model. Ranges of processing conditions have been identified that produce stable operation and thus effective pasteurisation of product.

Acknowledgement

This research was done as part of a PhD project supported by a BBSRC studentship in collaboration with Campden BRI (Gloucestershire, UK). The project is supported by the RCUK National Centre for Sustainable Energy Use in Food Chains: (EP/K011820/1). The authors would like to thank Revtech process systems (Loriol-sur-Drome, FR) for providing the equipment.

References

Almond Board of California, 2007. Considerations for Proprietary Processes Used for Almond Pasteurization and Treatment. Available: http://www.almonds.com/sites/default/files/content/attachments/proprietary-processes.pdf (Accessed: 04/2016).

Barrile, J.C., Cone, J.F., 1970. Effect of added moisture on the heat resistance of Salmonella anatum in milk chocolate. Appl. Microbiol. 19 (1), 177–178.

Beuchat, L., Komitopoulou, E., Betts, R., Beckers, H., Bourdichon, F., Joosten, H., Fanning, S., ter Kuile, B., 2011. Persistence and survival of pathogens in dry foods and dry food processing environments. Int. Life Sci. Inst. Eur. Rep. Ser. 1–48.

Beuchat, L.R., Komitopoulou, E., Beckers, H., Betts, R., Bourdichon, F., Fanning, S., Joosten, H., ter Kuile, B., 2013. Low-water activity foods: increased concern as vehicles of foodborne pathogens. J. Food Prot. 76 (1), 150–172.

Buhler AG, (2014). http://www.buhlergroup.com/northamerica/en/downloads/CCP.pdf (Accessed 04/2016).

Chang, S.-S., Han, A.R., Reyes-De-Corcuera, J.I., Powers, J.R., Kang, D.-H., 2010. Evaluation of steam pasteurization in controlling Salmonella serotype Enteritidis on raw almond surfaces. Lett. Appl. Microbiol. 50 (4), 393–398.

Chick, M., 2011. Thermal Inactivation Kinetics of Salmonella Serovars on Dry Cereal. M.S. thesis. Retrieved from the University of Minnesota Digital Conservancy. http://purl.umn.edu/116854.

Codex Alimentarius Commission, 2013. Proposed Draft Code of Hygienic Practice for Low-moisture Foods CX/FH 13/45/7. Food and Agriculture Organization of the United Nations, World Health Organization. Available: ftp://ftp.fao.org/codex/meetings/ccfh/ccfh45/fh45_07e.pdf (Accessed 04/2016).

ETIA(2014). "www.spirajoule.com." (Accessed 04/2016).

Harris, L.J., Uesugi, A.R., Abd, S., McCarthy, K.L., 2012. Survival of Salmonella Enteritidis PT 30 on inoculated almond kernels in hot water treatments. Food Res. Int. 45 (2), 1093–1098.

Heldman, D.R., 2011. Kinetic models for food systems. In: Food Preservation Process Design. Elsevier, Amsterdam, pp. 19–48.

Jeong, S., Marks, B.P., Orta-Ramirez, A., 2009. Thermal inactivation kinetics for Salmonella enteritidis PT30 on almonds subjected to moist-air convection heating. J. Food Prot. 72 (8), 1602–1609.

Keppler, S., Bakalis, S., Leadley, C.E., Fryer, P.J., 2015. A systematic study of the residence time of flour in a vibrating apparatus used for thermal processing. Innov. Food Sci. Emerg. Technol. 33, 462–471.

Lee, S.-Y., Oh, S.-W., Chung, H.-J., Reyes-De-Corcuera, J.I., Powers, J.R., Kang, D.-H., 2006. Reduction of Salmonella enterica Serovar Enteritidis on the surface of raw shelled almonds by exposure to steam. J. Food Prot. 69 (3), 591–595.

Mattick, K.L., Jorgensen, F., Legan, J.D., Cole, M.B., Porter, J., Lappin-Scott, H.M., Humphrey, T.J., 2000. Survival and filamentation of Salmonella enterica serovar enteritidis PT4 and Salmonella enterica serovar typhimurium DT104 at low water activity. Appl. Environ. Microbiol. 66 (4), 1274–1279.

Napasol(2015). "www.napasol.com." (Accessed 04/2016).

Neetoo, H., Chen, H., 2011. Individual and combined application of dry heat with high hydrostatic pressure to inactivate Salmonella and Escherichia coli O157:H7 on alfalfa seeds. Food Microbiol. 28 (1), 119–127.

Penaloza Izurieta, W., Komitopoulou, E., 2012. Effect of moisture on salmonella spp. heat resistance in cocoa and hazelnut shells. Food Res. Int. 45 (2), 1087–1092.

Podolak, R., Enache, E., Stone, W., Black, G., Elliott, P.H., 2010. Sources and risk factors for contamination, survival, persistance, and heat resistance of Salmonella in low-moisture foods. J. Food Prot. 73 (10), 1919–1936.

Revtech(2015). "http://www.revtech-process-systems.com/index.php/en/(Accessed 04/2016).

Silva, F.V.M., Gibbs, P.A., 2012. Thermal pasteurization requirements for the inactivation of Salmonella in foods. Food Res. Int. 45 (2), 695–699.

Villa-Rojas, R., Tang, J., Wang, S., Gao, M., Kang, D.-H., Mah, J.-H., Gray, P., Sosa-Morales, M.E., Lopez-Malo, A., 2013. Thermal inactivation of Salmonella enteritidis PT 30 in Almond Kernels as influenced by water activity. J. Food Prot. 76 (1), 26–32.